

Adaptive TDMA/OFDMA for Wide-Area Coverage and Vehicular Velocities

Mikael Sternad*, Sorour Falahati*, Tommy Svensson†, and Daniel Aronsson*

*Signals and Systems, Uppsala University, PO Box 528, SE-751 20 Uppsala, Sweden,

†Dept. Signals and Systems, Chalmers University of Technology, SE-41296 Göteborg, Sweden,
{mikael.sternad, sorour.falahati, daniel.aronsson}@signal.uu.se; tommy.svensson@s2.chalmers.se

Abstract— Within the EU FP6 Integrated Project WINNER, adaptive transmission is investigated as a key technology for boosting the spectral efficiency of a new radio interface for 4G systems. Adaptive allocation of time-frequency chunks in an OFDM-based system offers a significant potential, but also poses challenges. Within work package two of WINNER, we study critical issues such as the feasibility of adaptive transmission over fading downlink/uplink channels to/from vehicular terminals, the corresponding required channel prediction accuracy, and the required feedback control bandwidth. This paper summarizes recent results obtained within WINNER, and related results obtained within the Swedish Wireless IP project.

Index Terms—4G mobile wireless systems, adaptive transmission and multiple access, Orthogonal Frequency Division Multiplexing (OFDM), spectral efficiency.

I. INTRODUCTION

ADAPTIVE systems allocate (schedule) time, frequency and antenna resources based on channel quality and user requirements. They enable efficient resource utilization and multi-user scheduling gains, when channels to different terminals fade independently. In systems based on time division multiple access/ adaptive OFDM (TDMA/OFDMA), time-frequency resources (chunks) are allocated. This provides a flexible small-scale granularity of the resources, ideal for transmitting small as well as large packets. Based on the results obtained within the Swedish Wireless IP project¹, we are assessing the feasibility of such methods in novel broadband radio interfaces within the EU FP6 Integrated Project WINNER².

We here investigate adaptive downlinks and uplinks based on fast scheduling and link adaptation, also for users at vehicular speeds, with a non-adaptive fall-back mode for very fast moving users. The non-adaptive fallback mode design is outside the scope of this paper, but should be based on time, frequency and space diversity techniques. Allocation of fast

fading channels requires channel prediction. The signal to interference and noise ratio (SINR) is to be predicted for all potential resources in future transmission.

In the proposed downlink, each terminal predicts the SINR over a major part of the total bandwidth. All active terminals report source coded SINR values or source coded suggested modulation formats over a shared uplink control channel. A resource scheduler, located close to one or several radio access points, allocates the downlink resources.

In an adaptive uplink, one has the problem that channels from each potential user will have to be estimated and predicted. In a system using frequency division duplex (FDD), the estimation must be carried out in the access point, and has to be based on pilots transmitted by all active terminals. To avoid unacceptable pilot overhead, these pilots must be transmitted simultaneously, by overlapping pilots. This is related to the problem of estimating channels from multiple antennas [3]. There are four key problems in the system, and we investigate solutions to the first two of them in this paper:

1. Predicting the short-term fading over a large fraction of the wavelength at high carrier frequencies and high terminal velocities.
2. Obtaining a high channel prediction quality of uplinks for many active users with a low pilot overhead.
3. Achieving a low channel state feedback data rate in a system with large bandwidth and fine granularity of the chunks.
4. Maintaining a good frequency synchronization of all uplinks to avoid significant intercarrier interference.

II. FDD DOWNLINK AND UPLINK DESIGN

We explore adaptive TDMA/OFDMA designed at carrier frequency 5 GHz. Adaptive transmission to vehicular users over TDMA/OFDMA downlinks has earlier been investigated in [1] and [2] for a more narrowband system of 5 MHz bandwidth at carrier frequency 1.9 GHz and early results in the WINNER context with a different design are given in [5].

The basic time-frequency resource unit is denoted chunk. It consists of a rectangular time-frequency area that comprises a number of subsequent OFDM symbols and a number of

¹ www.signal.uu.se/Research/PCCwirelessIP.html

² This work has been performed in the framework of the IST project IST-2003-507581 WINNER, which is partly funded by the European Union. The authors would like to acknowledge the contributions of their colleagues.

adjacent subcarriers, and is allocated exclusively to one user data flow. In Table I, we show the assumed chunk size along with important system parameters. A chunk contains payload and pilot symbols. It may also contain control symbols to minimize feedback delays, i.e. in-band control signaling. The number of offered payload bits in a chunk depends on the utilized modulation and coding scheme (MCS), which is selected adaptively.

TABLE I
BASIC PARAMETERS FOR FDD WIDE-AREA DOWNLINK AND UPLINK

Centre frequency	5.0 +/- 0.384 GHz
Number of OFDM sub-carriers	1024
FFT BW	20.0 MHz
Signal BW	16.25 MHz paired
Number of used subcarriers	832
Sub-carrier spacing	19531 Hz
OFDM symbol length (excl. CP)	51.20 μ s
Cyclic prefix (CP) length	5.00 μ s
Physical chunk size	156.24 kHz x 337.2 μ s
Chunk size in symbols	8 x 6 = 48

A. Downlink

The downlink is designed as follows. Regular pilot patterns are transmitted on the downlink. Based on channel measurements up to chunk time i , all active terminals predict the channel quality in all chunks within a sub-band of interest at the future chunk time $i+2$. These reports are source-coded and transmitted on uplink control symbols within the uplink chunks at time $i+1$. The appropriate MCS that could be used by each terminal in each chunk is then determined based on SINR rate limits. The adaptive resource scheduler at the access point allocates each chunk at time $i+2$ exclusively to one of the flows. The allocation is reported by control symbols in the allocated downlink chunks at time $i+2$.

In each downlink chunk, four pilot symbols and eight in-band control symbols are assumed. MCSs ranging from BPSK rate $\frac{1}{2}$ to 64-QAM rate $\frac{5}{6}$ are used. Thus, the number of payload bits per chunk may vary between 18 and 180.

Let the subcarriers within a chunk be enumerated from $c=1-8$, and let the six OFDM symbols be enumerated from $s=1-6$, see Fig. 1 (left). Channel predictors utilize subcarriers 3 and 7, and the channel estimation can utilize the control symbols in a decision-directed mode.

Symbols $(c,s)=(3,1),(3,2),(7,1),(7,2)$ carry the downlink control bits, and determines which of the present chunks that belong to which flow. Coded 4-QAM symbols are used.

Symbols $(c,s) = (3,3)$ and $(7,3)$ are known uncoded 4-QAM pilots. At multi-antenna access points, different pilots are transmitted from each antenna. The pilots are used for two purposes: channel estimation for coherent detection within chunks with payload of interest and prediction for all frequencies of interest for future adaptive downlink transmission. When OFDM symbol 3 within chunk i has arrived, channel prediction for chunk $i+2$ is performed. The required prediction horizon to the end of chunk $i+2$ is $2.5 \times 0.3372 \text{ ms} = 0.843 \text{ ms}$.

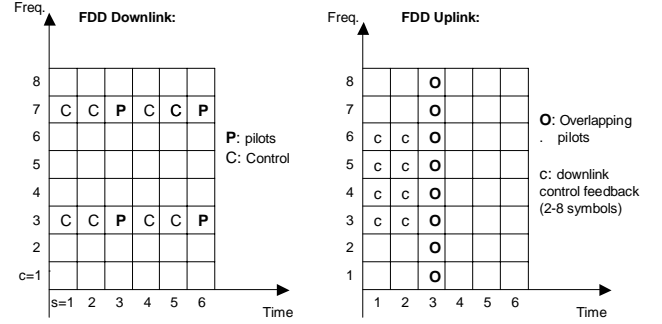


Fig. 1. Pilot and control symbol patterns in FDD downlink and uplink.

Symbols $(c,s) = (3,4), (3,5), (7,4)$ and $(7,5)$ carry control information for the next uplink transmission telling which of the next uplink chunks have been appointed to which uplink flow. Coded 4-QAM symbols are used.

Symbols $(c,s) = (3,6)$ and $(7,6)$ are known uncoded 4-QAM pilots, used for coherent detection and for updating the predictor states.

Control information is broadcast and has to be detectable by all users. Thus, their reception range essentially defines the cell radius. The control symbols are all located on the same subcarriers as the pilots, to make use of them for decision-directed channel estimation, in order to reduce the channel estimation mean square error (MSE) and the prediction MSE.

B. Uplink

On the uplink, terminals taking part in adaptive transmission are in competition for a part of the total 16.25 MHz band, called a *contention band*. All active terminals assigned to a contention band simultaneously send overlapping pilot signals during chunk time i . All eight symbols within OFDM symbol $s=3$ as shown in Fig.1 (right) are reserved for this purpose. Predictors located at the access point predict the channels for all terminals at time $i+2$. The prediction is based on the latest and previously received signals at the locations of the overlapping pilots. The appropriate MCS that could be used by each terminal in each chunk is then determined. The adaptive resource scheduler assigns the uplink transmission for time $i+2$ and informs the terminals by in-band signaling using control symbols of the downlink chunk at time $i+1$.

The in-band control symbols on the uplink which are positioned early in the chunk, see Fig. 1 (right), are part of the control loop for the downlink. They carry the downlink channel prediction reports from all active terminals. Their number (depending on the number of active terminals and their velocities) can be adapted to the requirements, varying from 1 to 8 coded 4-QAM symbols per chunk. The use of overlapping pilots in a Kalman filter that simultaneously estimates and predicts all channels is described in [6]. In multi-antenna receivers, the prediction should be performed separately for all receiving antennas within a sector/cell. The prediction horizon from symbol 3 in chunk i to the end of chunk $i+2$ is $2.5 \times 0.3373 \text{ ms} = 0.843 \text{ ms}$.

III. CHANNEL PREDICTION

The feedback loops for the FDD system is designed to be as fast as possible, under realistic constraints imposed by computation times and signaling delays. However, channel prediction is needed for scheduling and link adaptation, since extrapolating the present channel estimate would lead to large performance losses.

Extensive investigations of channel power predictors were performed in e.g. [7], [8] and [9]. Both theoretical analyses and evaluations on a large set of measured channels with 5 MHz bandwidth were taken into account. It was concluded that the class of channel power predictors that performed best on measured data was based on linear prediction of the complex baseband channel, followed by use of a quadratic unbiased predictor to predict the channel power. The noise level was found to be the crucial limiting factor for the attainable performance accuracy. Schemes that utilize many samples to average and suppress noise will provide better prediction performance. It is therefore advantageous for the prediction performance if a large fraction of symbols within the subcarriers are either pilots, or can be used for decision-directed estimation, as discussed also in section II.

In [7], the most significant taps of the channel impulse response are predicted in the time domain. Here, we instead do the prediction in the frequency domain. A set of linear prediction filters, each responsible for its own subband of the total bandwidth, is utilized³. The state space algorithm described in [4] is used to predict the complex channel and the unbiased quadratic predictor is used to predict the channel power. The algorithm in [4] starts by deriving a Kalman predictor. The predictor utilizes the correlation of the channel in the frequency domain by predicting p pilot-containing subcarriers in parallel. It also utilizes the correlation in the time domain of the fading channel. The number p is a compromise between performance and computational complexity. We use $p = 8$, spanning 4 chunks. This means that 26 such Kalman estimators would be required to cover a complete band of 104 chunks in both cases.

In [4] it is shown that the present OFDM channel prediction problem is ideally suited to the application of a novel low-complexity approximation of the Kalman algorithm, the Generalized Constant Gain algorithm [10], which avoids the need to update a quadratic state-space Riccati difference equation, responsible for the dominant computational load in Kalman algorithms.

Autoregressive models of order 4 are used to model the channel correlation in time. They are adjusted to the fading statistics. The state update equations of the Kalman/GCG estimators are based on these models.

In FDD uplinks, channel prediction is performed at the access point, using overlapping pilots from the terminals. A generalization of the Kalman algorithm of [4], described in [6], is used. Its performance is investigated below.

³ Comparative evaluations of the frequency domain and the time domain approach are currently underway within the Swedish Wireless IP project.

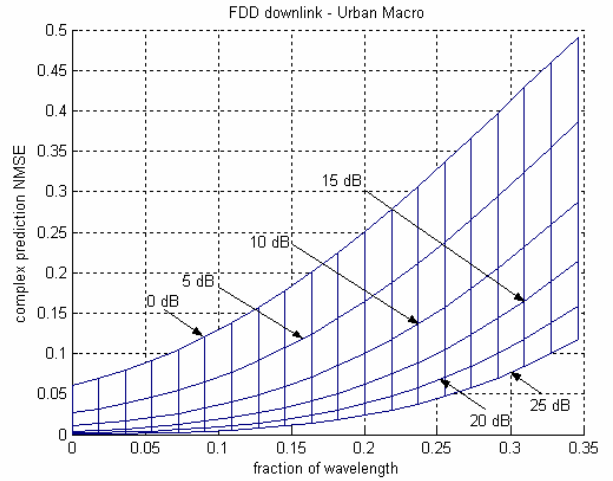


Fig. 2. Normalized prediction error, as a function of the prediction horizon scaled in carrier wavelengths, and as function of the SINR. Results for FDD downlink, full duplex terminals, over WINNER Urban Macro channels, with a Kalman algorithm utilizing 8 subcarriers.

TABLE II
WINNER URBAN MACRO POWER DELAY PROFILE

$\tau_n = \{0, 10, 30, 250, 260, 280, 360, 370, 385, 1040, 1045, 1065, 2730, 2740, 2760, 4600, 4610, 4625\}$ ns	$p_n = \{-3, 5.22, 6.98, 4.7184, 6.9384, 8.6984, 5.2204, 7.4404, 9.2004, 8.1896, 10.4096, 12.1696, 12.0516, 14.2716, 16.0316, 15.5013, 17.7213, 19.4813\}$ dB
---	---

IV. PERFORMANCE RESULTS

A. Frequency domain Kalman/GCG channel prediction

The FDD downlink with WINNER Urban Macro power delay profile, defined in Table II, and white noise with known power are used in the investigation of the prediction error as a function of the prediction horizon, scaled in wavelengths, for different values of the SINR. Fig. 2 shows the results for full duplex terminals using all timeslots for updating the predictor with measurements. There is a large sensitivity to SINR, and the prediction error grows with the prediction horizon. The results for prediction horizon zero represent the filter NMSE.

Fig. 3 shows results for FDD uplinks, where 2 users and 8 users respectively are simultaneously transmitting overlapping pilots, all having the same average received power. In a Kalman estimator based on overlapping pilots, separate sets of states are used for describing the channel of each user. The autoregressive models that describe the fading statistics of each user are adjusted individually to the velocity of the users [6]. Uplink control information could be used for improving the estimate by decision-directed methods, but it is not used in the presented results. All users have the same velocity and travel through the same type of propagation environment, but with independent channel realizations. These results are based on the ITU Vehicular-A channel model. The average received power is assumed equal for all users (slow power control). The results indicate that prediction based on overlapping pilots will decrease in accuracy with an increasing number of terminals, but this decrease is rather modest. Channel predictions in FDD uplinks in which not too many users occupy each contention band thus seems feasible.

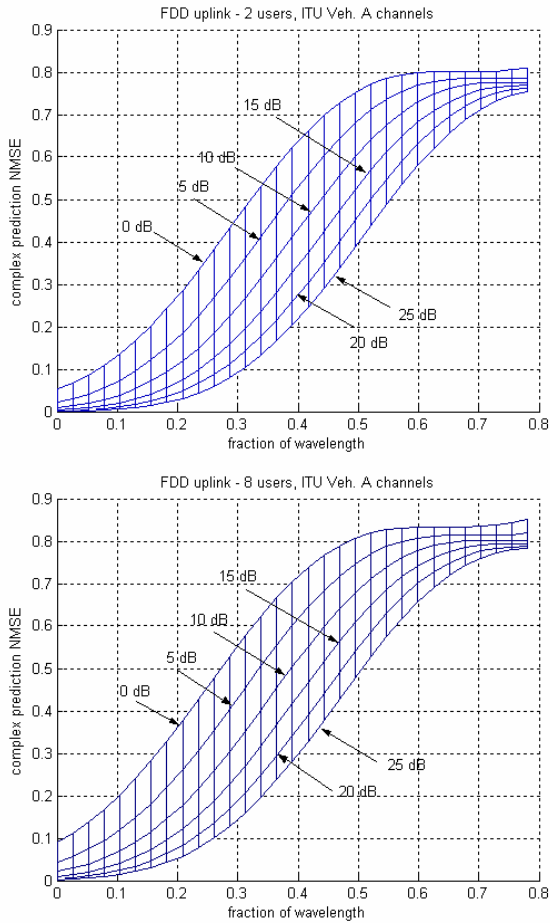


Fig. 3. Normalized prediction error of the prediction horizon scaled in carrier wavelengths, and as function of the SINR. Results for FDD uplink over ITU Vehicular-A channels, with a Kalman algorithm for overlapping uplink pilots utilizing 8 subcarriers. Result for 2 (top) and 8 (bottom) simultaneous users per contention band.

B. Limits for adaptive FDD TDMA/OFDMA transmission

The prediction accuracy depends on the prediction horizon h scaled in wavelength, which in turn depends on the velocity v , the prediction horizon in time D and the carrier wavelength λ via the relation $h = vD / \lambda$. The prediction accuracy also depends on the SINR. Thus, adaptive transmission to/from a terminal will be feasible up to a maximal velocity for a given SINR, or equivalently, down to a limiting SINR at a given velocity. Estimates of the limiting SINR values are given here, based on the design in section II and the results in Fig. 2-3. They are conservative, since the prediction is performed to the far end of the chunk to be allocated. The prediction accuracy to less distant symbol locations will be higher.

From earlier investigations of the sensitivity for MCS rate limits to prediction errors, it has been found that if the rate limits are adjusted to take the prediction uncertainty into account, a prediction NMSE of 0.1 for an uncoded system leads to only a minor degradation in the spectral efficiency [11], [12], but for coded schemes the sensitivity to prediction errors is slightly larger. We here use an upper limit of 0.15 for the allowed normalized variance of the complex prediction error. Table III shows the resulting limits for the SINR along with the corresponding prediction horizons in wavelengths for

the prediction horizon $D = 0.843$ ms as required in section II for both downlink and uplink. It is evident that adaptive transmission can be expected to work in the widest variety of situations in the wide-area FDD downlinks, whereas adaptive transmission in the wide-area FDD uplink, can work in many important situations.

TABLE III
ESTIMATES OF THE SINR LIMITS FOR ADAPTIVE TRANSMISSION AT 5 GHz
WITH PREDICTION HORIZON IN WAVELENGTHS

SINR, prediction horizon	30 km/h	50 km/h	70 km/h
Downlink	< 0 dB, 0.117λ	6 dB, 0.195λ	12.5 dB, 0.273λ
Uplink, 2 users	0 dB, 0.117λ	7 dB, 0.195λ	15 dB, 0.273λ
Uplink, 8 users	3.5 dB, 0.117λ	11 dB, 0.195λ	20 dB, 0.273λ

V. SIMULATION RESULTS FOR FDD DOWNLINK

In this section, the SINR limits stated in Table III are compared to the simulation results of the adaptive FDD TDMA/OFDMA downlink using the WINNER Urban Macro model. In the multilink simulations, all channels have the same statistical properties, all terminals are full duplex and have the same velocity. The interference is modeled with white Gaussian noise and all terminals have the same average SINR.

The scheduling strategy used is Proportional Fair, which in this case, where all users have the same average SINR, reduces to the Max Throughput strategy of giving the chunk to the user who can use the highest modulation-coding rate. The resource scheduling buffers are never emptied.

The channels are not perfectly flat within the chunks: there is in general variability both in the time direction and in the frequency direction. Within each chunk, the modulation and coding scheme potentially used by each user is determined by taking the average predicted SINR, $SINR_{av}$, and the predicted SINR at the worst point within the chunk, $SINR_w$, for that user. The weighted average is used as the effective SINR: $SINR[dB] = bSINR_{av}[dB] + (1-b)SINR_w[dB]$.

The parameter b can be used to tune the performance of the scheme when we have significant channel variability within the chunks. With $b=1$, large variability leads to a large increase in the BER, since the properties of the worst corner of the chunk generates most errors. With $b=0$, we obtain a conservative scheme, that tends to provide on average less errors than the target BER. In all results shown, $b=0.4$ is used. The effect of channel estimation errors on the demodulation is not considered.

As scheduling unit (SU), we use 512-bit packets (small IP packet). The overhead due to CRC code and sequence numbers for link ARQ is not taken into account. Each SU is distributed among the allocated chunks, and superfluous payload symbols are filled with zeros. Separate MCS is used for each chunk. If all bits belonging to a SU are received correctly, it is released to higher layers. Otherwise, a link

retransmission would occur. However, link level retransmission is not used in the simulations.

Coded M-QAM are used with eight rates: BPSK rate $\frac{1}{2}$, QPSK rate $\frac{1}{2}$, QPSK rate $\frac{3}{4}$, 16-QAM rate $\frac{1}{2}$, 16-QAM rate $\frac{2}{3}$, 16-QAM rate $\frac{5}{6}$, 64-QAM rate $\frac{2}{3}$ and 64-QAM rate $\frac{5}{6}$, based on the rate $\frac{1}{2}$ constraint length 9 convolutional code with generator polynomials (561,753) in octal representation, which is punctured to obtain the higher rate codes. The rate limits are optimized under a maximal bit error rate constraint of 0.001, for a given average SINR and prediction error variance. The actual average bit error rate becomes lower, since the maximal BER is targeted for the MCS limits.

The throughput is defined as the number of payload bits in correctly received SUs divided by the total number of transmitted payload symbols. The effect of different terminal velocities and the corresponding prediction uncertainties on the throughput, the multiuser scheduling gain and the bit error rate are measured.

Table III indicates that when all users have either 10 dB SINR or 19 dB SINR, the adaptation scheme should work rather well for all velocities up to 70 km/h at 19 dB, but difficulties may be encountered at 70 km/h when the SINR is 10 dB. Fig. 4 confirms this statement. The dashed curves show the performance in the presence of prediction inaccuracy. The solid curves show the case when predictions are assumed perfect, but the effect of the channel variability within chunks due to the fading in time is taken into account.

For the dashed curves, the MCSs are designed to attain the BER constraints in the presence of prediction errors. This goal is fulfilled, with one exception: that of 70 km/h at 19 dB SINR. The corresponding packet error rates for the 512 bit SU is below 1%, which indicates that performance could be improved by tuning the scheme more aggressively. With an increasing speed, and correspondingly increasing prediction uncertainty, the rate limits are tuned more conservatively, and the throughput is decreased. Significant multiuser scheduling gains are however preserved also with rather long predictions.

At 70 km/h and 10 dB SINR the scheme fails due to too high prediction uncertainty, and this operating point is beyond the limit given in Table III. Note also that the prediction uncertainty decreases with the number of active users since with many users, chunks are given to users with relatively good channels having a small prediction uncertainty.

With the results above, we have shown that it is possible to adaptively utilize the short-term fading also for vehicular users at such high carrier frequencies as 5 GHz.

REFERENCES

- [1] W. Wang, T. Ottosson, M. Sternad, A. Ahlén and A. Svensson, "Impact of multiuser diversity and channel variability on adaptive OFDM," VTC 2003 Fall, Orlando, FL, Oct. 2003.
- [2] M. Sternad, T. Ottosson, A. Ahlén and A. Svensson, "Attaining both coverage and high spectral efficiency with adaptive OFDMA downlinks," VTC 2003-Fall, Orlando, Fla, Oct. 2003.
- [3] G. Auer, "Analysis of pilot-symbol aided channel estimation for OFDM systems with multiple transmit antennas", IEEE ICC 04, Paris, June 2004.

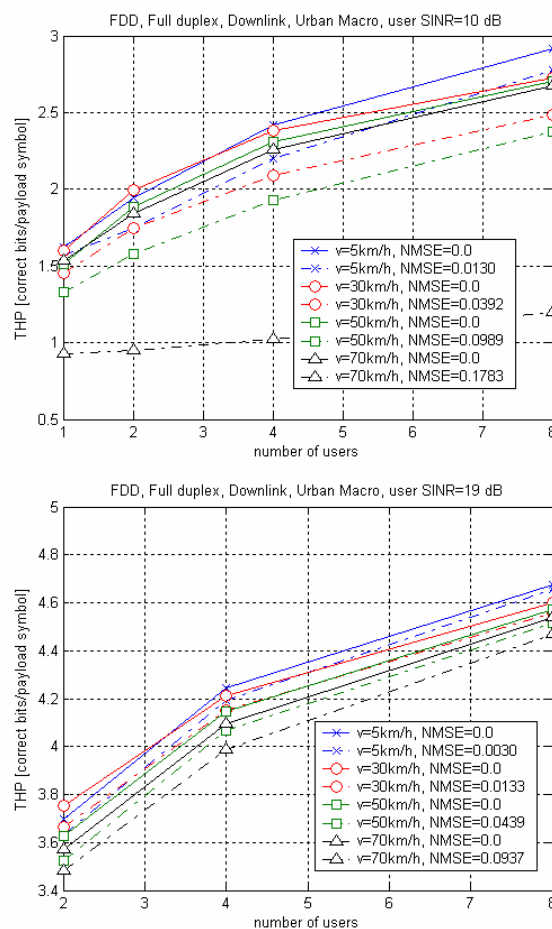


Fig. 4. Throughput as a function of the number of active users, all with the same average SINR of 10 dB (top) and 19 dB (bottom) in FDD wide-area downlink. Solid curves take channel variability within chunks into account but neglect the prediction uncertainty. Dashed curves take prediction uncertainty into account.

- [4] M. Sternad and D. Aronsson, "Channel estimation and prediction for adaptive OFDM downlinks," IEEE VTC 2003-Fall, Orlando, Fla, Oct. 2003.
- [5] M. Sternad, S. Falahati and T. Svensson. "Adaptive OFDMA/TDMA Transmission at Vehicular Velocities". Proc. Wireless World Research Forum WWR12, Toronto, Canada, Nov 2004.
- [6] M. Sternad and D. Aronsson, "Channel estimation and prediction for adaptive OFDMA/TDMA uplinks, based on overlapping pilots", International Conference on Acoustics, Speech and Signal Processing (ICASSP 2005). Philadelphia, PA, USA, March 19-23 2005. Online: <http://www.signal.uu.se/Publications/abstracts/c0501.html>
- [7] T. Ekman, Prediction of Mobile Radio Channels. Modelling and Design. Ph.D. Th., Signals and Syst., Uppsala Univ. <http://www.signal.uu.se/Publications/abstracts/a023.html>
- [8] M. Sternad, T. Ekman and A. Ahlén, "Power prediction on broadband channels", IEEE Vehicular Technology Conference VTC01-Spring, Rhodes, Greece, May 6-9 2001.
- [9] T. Ekman, M. Sternad and A. Ahlen, "Unbiased power prediction on broadband channels" IEEE VTC 2002-Fall, Vancouver, Canada, Sept. 2002.
- [10] M. Sternad, L. Lindbom and A. Ahlén, "Wiener design of adaptation algorithms with time-invariant gains," IEEE Transactions on Signal Processing, vol. 50, pp. 1895-1907, August 2002.
- [11] S. Falahati, A. Svensson, T. Ekman and M. Sternad, "Adaptive modulation systems for predicted wireless channels," IEEE Trans. on Communications, vol. 52, Feb. 2004, pp. 307-316.
- [12] S. Falahati, A. Svensson, M. Sternad and H. Mei, "Adaptive Trellis-coded modulation over predicted flat fading channels," IEEE VTC 2003-Fall, Orlando, Fla, Oct. 2003.